

METHODS OF DECREASING LOSSES IN OPTICAL METAMATERIALS

**Zoran Jakšić¹, Marko Obradov¹, Olga Jakšić¹, Goran Isić^{2,3},
Slobodan Vuković^{1,3}, Dana Vasiljević Radović¹**

¹Center of Microelectronic Technologies, Institute of Chemistry, Technology and Metallurgy, University of Belgrade, Njegoševa 12, 11000 Belgrade, Serbia

²Institute of Physics, University of Belgrade, Pregrevica 118, 11080 Belgrade, Serbia

³Science program, Texas A&M University at Qatar, P.O. Box 23874 Doha, Qatar

Abstract. *In this work we review methods to decrease the optical absorption losses in metamaterials. The practical interest for metamaterials is huge, but the possible applications are severely limited by their high inherent optical absorption in the metal parts. We consider the possibilities to fabricate metamaterial with a decreased metal volume fraction, the application of alternative lower-loss plasmonic materials instead of the customary utilized noble metals, the use of all-dielectric, high refractive index contrast subwavelength nanocomposites. Finally, we dedicate our attention to various methods to optimize the frequency dispersion in metamaterials by changing their geometry and composition in order to reach lower absorption, which includes the use of the hypercrystals. The final goal is to widen the range of different metamaterial-based devices and structures, including those belonging to transformation optics. Maybe the most important among them is the fabrication of a novel generation of all-optical or hybrid optical/electronic integrated circuits that would operate at optical frequencies and at the same time would offer a packaging density and complexity of the contemporary integrated circuits, owing to the strong localization of electromagnetic fields enabled by plasmonics.*

Key words: *Metamaterials, Transformation Optics, Plasmonics, Low-Loss Metamaterials, Hyperbolic metamaterials*

1. INTRODUCTION

Artificial structuring of optical materials at the subwavelength level ensures excellent control over spectral and spatial dispersion. It becomes possible to obtain very high, very low (near-zero) and negative effective values of refractive index. A path is thus opened to tailoring

Received August 22, 2018

Corresponding author: Zoran Jakšić,

Institute of Chemistry, Technology and Metallurgy, University of Belgrade, Njegoševa 12, 11000 Belgrade, Serbia

(E-mail: jaksa@nanosys.ihtm.bg.ac.rs)

the optical space at will, ultimately leading to the new field of transformation optics, Fig. 1 [1-3].

The materials structured in the quoted manner possess electromagnetic properties that surpass those normally met in nature and are thus denoted as metamaterials [4, 5]. In a general case, metamaterials represent 1D, 2D or 3D composites of constituent parts with different values of complex refractive index, Fig. 2, and are the main building blocks for tailoring the optical space. They are typically structured at a subwavelength level, which in the case of visible radiation is of the order of nanometers. In most cases the optical metamaterials owe their operation to electromagnetic localization on an interface between the two constituent materials (typically metal and dielectric). In such a situation an evanescent wave is formed at the interface, called surface plasmon polariton. In its basic form such a surface wave is obtained by coupling free electron plasma in the metal part with the P-polarized electromagnetic wave at the interface between semi-infinite dielectric and semi-infinite metal. Depending on geometry of the nanocomposite and its constituent materials, a host of different waves can appear at the surface and in the bulk [6-8]. The strong localization of the electromagnetic field at the surface lies in the root of many exotic optical phenomena connected with plasmonic metamaterials.

Many novel wave phenomena are met in such metastructures, for instance extreme light concentration [9, 10], near-perfect absorption [11-13], superlensing [14-16] and hyperlensing [17-19], optical cloaking (invisibility shields) [3, 20, 21], to name just a few. Basically, using metamaterials anything could be done with propagation of electromagnetic waves, the practical limit being only the imagination.

One of the most interesting practical goals of metamaterials and transformation optics is merging the packaging density of electronic devices with the speed of photonic ones by creating ultracompact, all-optical circuits as a new step in the continuation of the Moore's law [22]. This holds the potential to revolutionize the electronics industry.

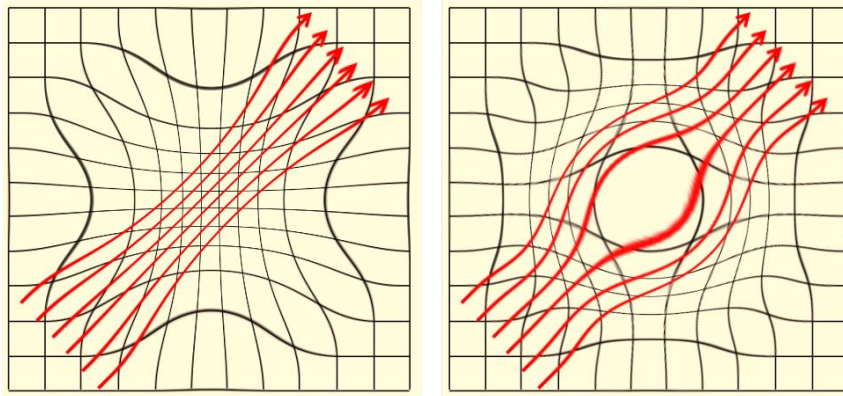


Fig. 1 Modification of the optical space by transformation optics. Black lines represent the optical space (the artificially made structure of the metamaterial) while red arrows show the propagation of electromagnetic beams.

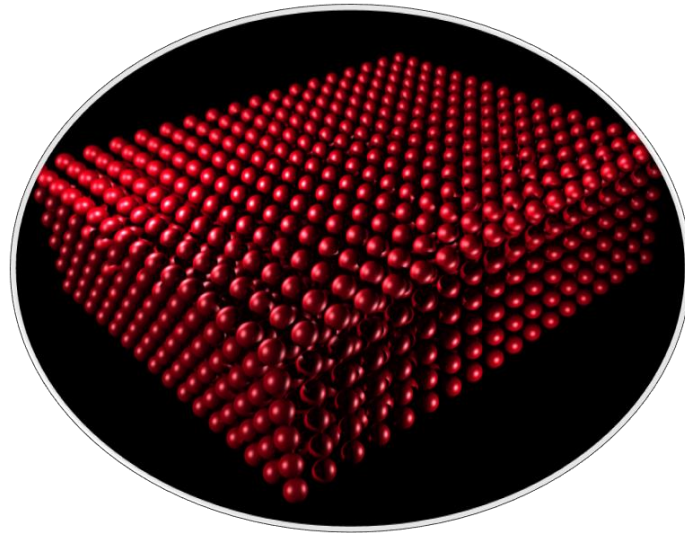


Fig. 2 An example of 3D structuring of optical metamaterials (spheres with a given value of complex refractive index within a host with a different refractive index.)

To obtain extreme concentrations, the typical approach is to utilize electromagnetic resonances in metal-dielectric nanocomposites, thus ensuring field localization at metal-dielectric interface (the already mentioned surface plasmons polaritons, SPP) [23].

The use of metals means high absorption losses, thus short propagation paths and generally poor figures of merit. This is a major obstacle to the more widespread application of transformation optics. A host of practical applications would benefit from low-loss plasmonics and nanophotonics.

In this work we consider strategies for nanostructuring of artificial optical composites to decrease or eliminate absorption. Some approaches include

- *Low metal volume fraction*: utilize structures with smaller relative amount of metal – generalization of the old concept of artificial dielectrics.
- *Alternative plasmonic materials*: use of plasmonic materials with lower losses compared to pure metals.
- *All-dielectric meta-optics*: completely avoid the use of metals and limit the design to pure dielectric and possibly low-loss semiconductors.
- *Optimizing frequency dispersion*: design metal-dielectric or even metal-metal nanocomposites with a frequency dispersion specifically tailored to obtain lower losses.

In the next sections we consider each of the quoted strategies.

2. LOW METAL VOLUME FRACTION

An obvious approach to decrease the absorption losses in metal-dielectric nanocomposites is to decrease their metal to dielectric volume fraction. Basically, this idea leans heavily on the concept of artificial dielectrics, used already in 1950ties in microwave technique [24, 25].

Here we have a simple rule of thumb, which also follows the common sense: as the metal volume fraction decreases, a smaller part of the wave propagates through the absorptive medium, thus losses become lower. On the other hand, field localization also tends to become weaker and the electromagnetic field spreads over a larger volume, see Fig. 3. Therefore, there is need for a trade-off between the two.

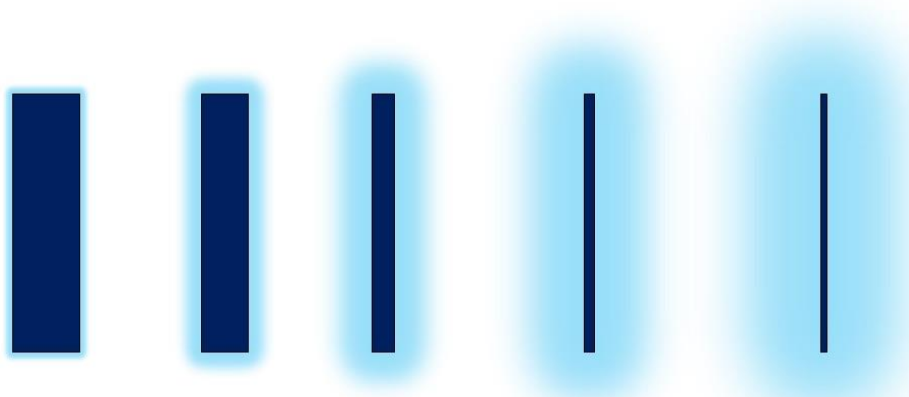


Fig. 3 Electromagnetic field distribution (light color) around metal/plasmonic material (dark color).

Figure 4. shows some examples of low metal fraction metamaterials. The top left structure is a one-dimensional plasmonic crystal [26] (metal-dielectric multilayer) with metal sheets much thinner than their dielectric counterparts. The top right structure in Fig. 4 is the simplest 1D plasmonic crystal, a freestanding metallic/plasmonic material membrane with nanometer thickness. The dielectric part of this plasmonic crystal is the surrounding ambient and it ensures a perfect electromagnetic symmetry of the structure – the dielectric above and below is identical.

As mentioned in the description of Fig. 4, the plasmonic nanomembrane [27, 28] is a typical example of 1D plasmonic structure with minuscule volume fraction of metal. It can be defined as a freestanding metallic (or generally material containing free electron plasma) structure with an extremely high aspect ratio (lateral dimensions being even several million times larger than the thickness which can be of the order of tens of nanometers, even less).

The thinner nanomembranes are, the longer are the propagation paths of SPP. This makes them an ideal platform for long-range surface plasmons polaritons [29, 30].

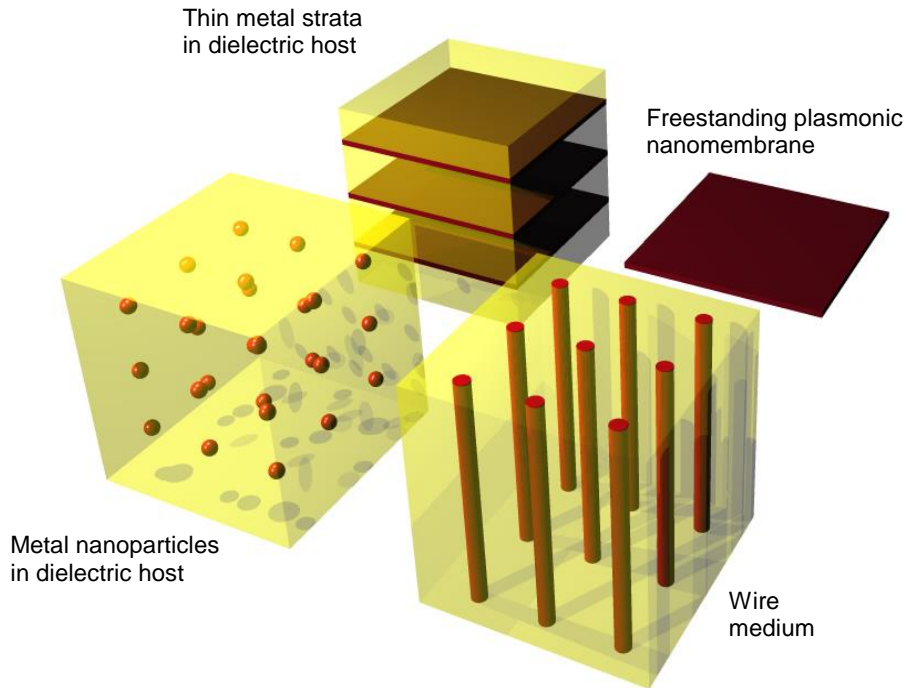


Fig. 4 Examples of plasmonic crystal-based metamaterials with low volume fraction of metal constituent. Top left: conventional metal-dielectric multilayer (1D plasmonic crystal – PC); top right: freestanding metal nanomembrane as the simplest 1D PC; bottom right: wire medium (metal wires within a dielectric host, 2D PC) and bottom left: metal/plasmonic particles within dielectric host (3D PC).

Propagation of SPP on separate interfaces of a membrane is shown in Fig. 5. When interfaces are close enough to each other (sufficiently thin membrane), separate SPP modes couple across the plasmonic membrane. If membrane becomes thinner still, two SPP modes merge into one.

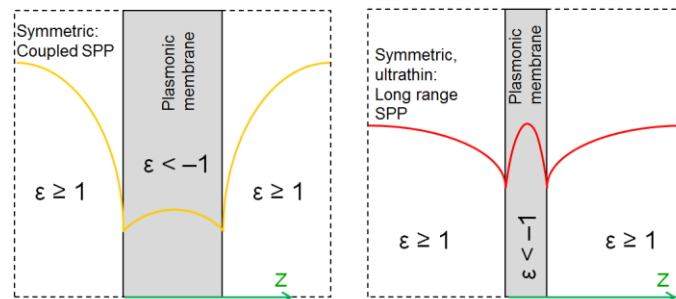


Fig. 5 Coupled SPP on membranes in IMI (insulator-metal-insulator) configuration.

3. ALTERNATIVE PLASMONIC MATERIALS

Plasmonic effects were usually obtained using good metals like gold and silver. At the same time, these materials have very strong absorption losses. In the recent years, however, the focus of attention has shifted to alternative plasmonic materials [31, 32] which also have free electron plasma, but they offer various advantages like tailorability of their electromagnetic response, lower absorption losses.

Probably the most interesting group of alternative plasmonic materials are optically transparent, electrically conductive oxides (TCO) [33]. Heavy doping ensures an increase of the electron concentration in these materials, thus contributing to an improvement of their plasmonic properties and at the same time ensuring tailoring of their spectral characteristics, i.e. shifting them to the near-infrared part of the spectrum. Examples of TCO include ITO – indium-tin-oxide; AZO – aluminum-zinc-oxide; GZO – gallium-zinc-oxide. Recently, however, it has been noted that the quoted properties come for a price and that the TCO figure of merit (the ratio of the real by imaginary part of the refractive index) reaches rather poor values, even worse than in noble metals they are intended to replace [7].

Other alternative plasmonic media include metallic alloys. They are tunable by design, by simply adjusting the alloy composition. Such tailoring could shift the peak losses to another frequency, possibly outside the operating range. This group of materials includes noble-transition alloys (e.g. Au-Cd), alkali-noble inter-metallic compounds (e.g. Li_2AgIn , KAu) and intermetallics (e.g. Ag_3Sn , Cu_3Sn). In spite of the tailorability of the composition of metal alloys and thus of their frequency dispersion, a problem of their excessively high absorption at optical wavelengths still remains, only mitigated to a minuscule degree.

Graphene represents weakly corrugated sub-nanometer honeycomb lattice of carbon. Its relatively low optical absorption in visible and infrared (of the order of 3%), connected with the existence of quasi-2D free electron plasma makes it a convenient candidate for plasmonics [34]. Its properties are easily tailored by doping and gating. A combination of graphene with noble metal nanoparticles has been proposed as a platform for tunable SPP [35]. Graphene plasmonics represents a field of its own and vastly surpasses the scope of this article.

Finally, an alternative plasmonic platform are highly doped semiconductors, e.g. GaAs, GaP, SiC, GaN, which also have free electron plasma. Their use in active and ultrafast plasmonics has been considered [36]. However, absorption losses in the visible are again a hurdle towards more widespread use.

4. ALL-DIELECTRIC META-OPTICS

The idea with all-dielectric metamaterials is to avoid absorption by completely removing lossy parts [37-39]. The price to pay is a lower degree of design freedom (it is far easier to localize EM field using metal-dielectric interfaces).

No metals or similar materials with free electron plasma are used: material can be pure dielectric or possibly semiconductor (simultaneously ensuring high refractive index and low losses). It is necessary to reach high refractive index contrast between scatterers and the embedding host.

Mie resonance theory [40] is applied (exact solution of the classical electromagnetic diffraction problem): both scatterer size and morphology/shape are important. Extreme

field concentration is obtained through creation of hotspots (nonlocalities) at deep subwavelength level due to edge effects at sharp angles. To achieve this the shapes of scatterers are modified. Some 3D shapes of nanoparticles are presented in Fig. 6; this is only a very small number of examples among a vast variety of the existing forms. Deep subwavelength hotspots cause effective medium approximation (EMA) to break down (conventional EMA theory no longer remains valid).

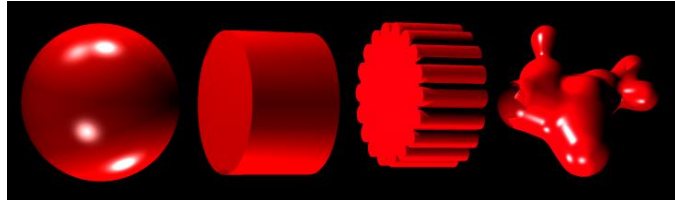


Fig. 6 Illustration of nanoparticles with different shapes.

Since resonances are shape-dependent, a wealth of new modes appears. Morphology-dependent EM behavior includes both electric and magnetic dipole resonances and higher order multipole resonances. In addition to that, relative positions of nanoparticles are important because magnetic or electric field tend to concentrate between them (nanoparticle dimers), again causing the appearance of magnetic or electric hotspots.

As an illustration, the scattering properties of a single all-dielectric cylinder on a substrate are shown in Figs. 7–8. The nanocylinders are on a low index substrate ($n=2$) surrounded by air and are built of a high index material ($n=8$). The cylinder radius is 50 nm and its height is 40 nm.

The scattering properties of all-dielectric nano-cones are shown in Figs. 9–12. The cones are deposited on a low index substrate ($n=1.5$) are surrounded by air and consist of a high index material ($n=4$). The dielectric cone base radius is 75 nm and the height is 100 nm.

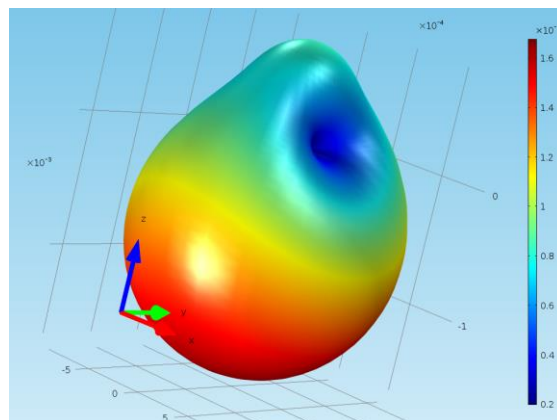


Fig. 7 Radiation pattern of far field scattered from a dielectric cylinder $h=40$ nm, $r=50$ nm, $n=8$ on a substrate $n=2$. The incident beam $\lambda=560$ nm arrives from above, along the cylinder axis.

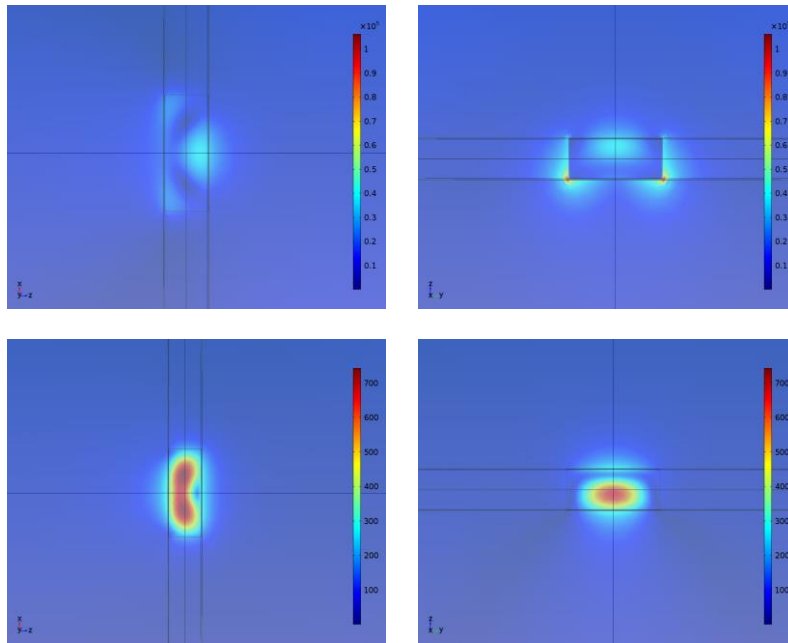


Fig. 8 Spatial distributions of field intensity; electric field (top row) and magnetic field (bottom row) for a dielectric cylinder $h=40$ nm, $r=50$ nm, $n=8$ on a substrate $n=2$ at $\lambda=560$ nm.

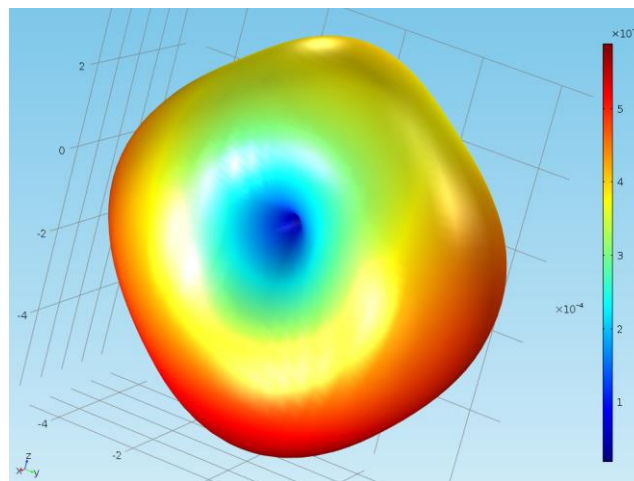


Fig. 9 Radiation pattern of far field scattered from a dielectric cone $h=100$ nm, $r=75$ nm, $n=4$ on a substrate $n=1.5$. The incident beam $\lambda=300$ nm arrives from above, along the axis of the cone.

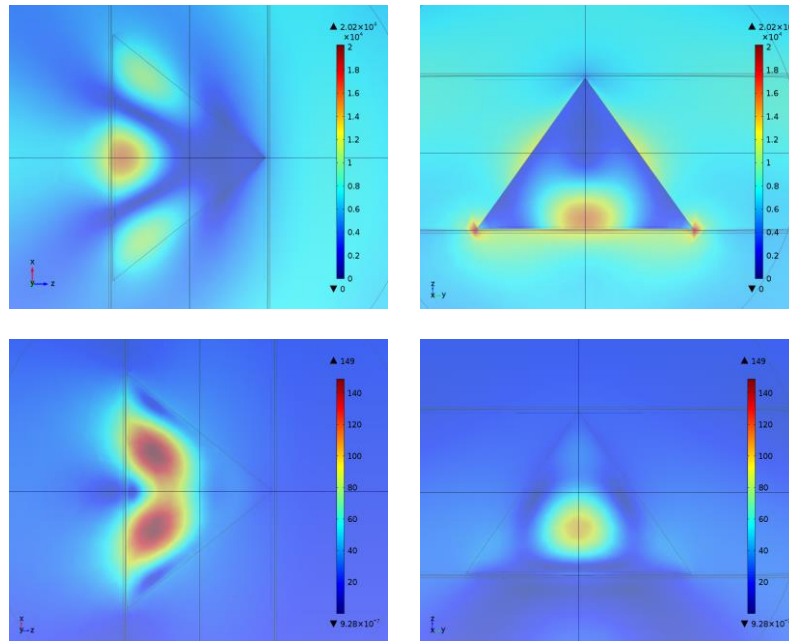


Fig. 10 Spatial distributions of field intensity; electric field (top row) and magnetic field (bottom row) for a dielectric cone $h=100$ nm, $r=75$ nm, $n=4$ on a substrate $n=1.5$. at $\lambda=300$ nm.

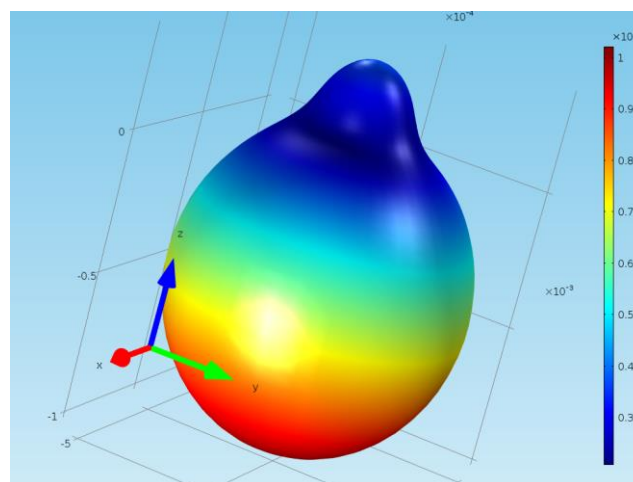


Fig. 11 Radiation pattern of far field scattered from a dielectric cone $h=100$ nm, $r=75$ nm, $n=4$ on a substrate $n=1.5$. The incident beam $\lambda=380$ nm arrives from above, along the axis of the cone.

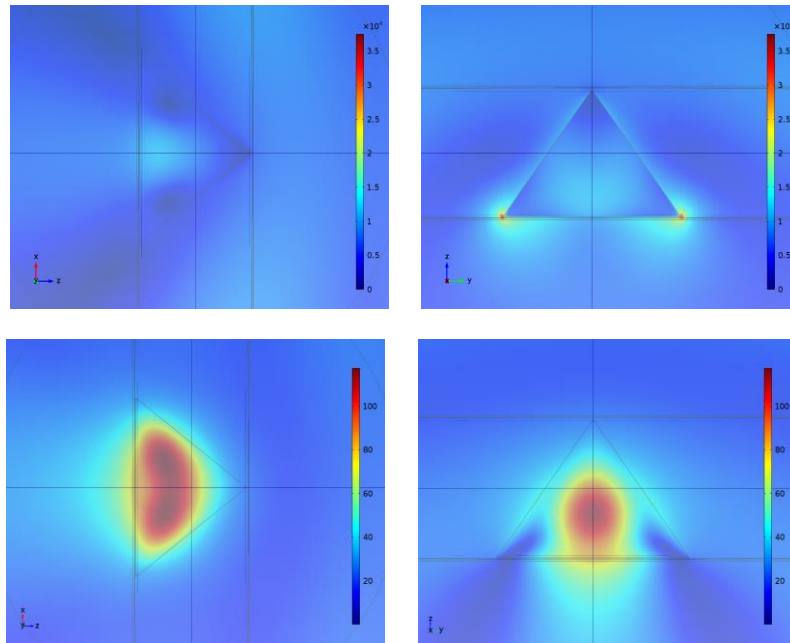


Fig. 12 Spatial distributions of field intensity; electric field (top row) and magnetic field (bottom row) for a dielectric cone $h=100$ nm, $r=75$ nm, $n=4$ on a substrate $n=1.5$. at $\lambda=380$ nm.

When deposited on an interface between two materials with different refractive indices single dielectric particle exhibits high directivity in its radiation pattern in favor of material with higher refractive index i.e. the substrate, same as with metallic particles [41, 42]. Unlike metals, electric field localizations occur also within the particle but are still tied to edges of the particle with much lower efficiency in comparison to metals. However, unlike metals, dielectric particles exhibit high magnetic field localizations within the particles with spatial distributions almost complementary to those of electric fields.

Figure 13 shows the response of purely dielectric nanodimers (paired nanocylinders, top view) [38]. For the field directions as in Fig. 13 the dimers exhibit field hotspots in the gap between the nanoparticles: for the electric field directed along the axis of the dimer a hotspot of the electric field appears, and for the magnetic field along the same axis a magnetic hotspot appears. In the case when the nanoparticles are metallic, an identical situation is encountered if the layout is as shown in Fig. 13a. However, metallic dimers behave oppositely to the dielectric ones when the configuration shown in Fig. 13b is used, and contrary to the all-dielectric case no magnetic hotspot appears at all.

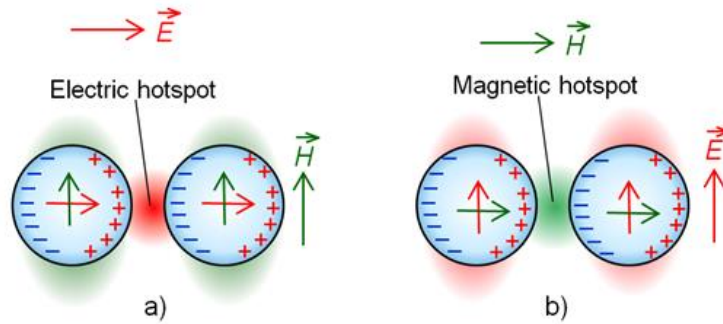


Fig. 13 Electric and magnetic hotspots in purely dielectric dimers. + and – signs describe polarization of molecules within dimers. The vector of electric polarization within separate nanoparticles has the same direction as the electric field, while magnetic polarization follows the magnetic field.

A square array of cylindrical high refractive index dielectric resonators is shown in Fig. 14. Such structure is denoted as dielectric Huygens metasurface [43]. A metasurface can be defined as quasi-2D structure with a subwavelength thickness containing metamaterial “atoms” in its plane, which are themselves with subwavelength dimensions. A Huygens metasurface can behave as a reflectionless plane, i.e. an array of Huygens sources which do not have a backward component of scattering. The metamaterial “atoms” in this case are high-index cylinders arranged in plane.

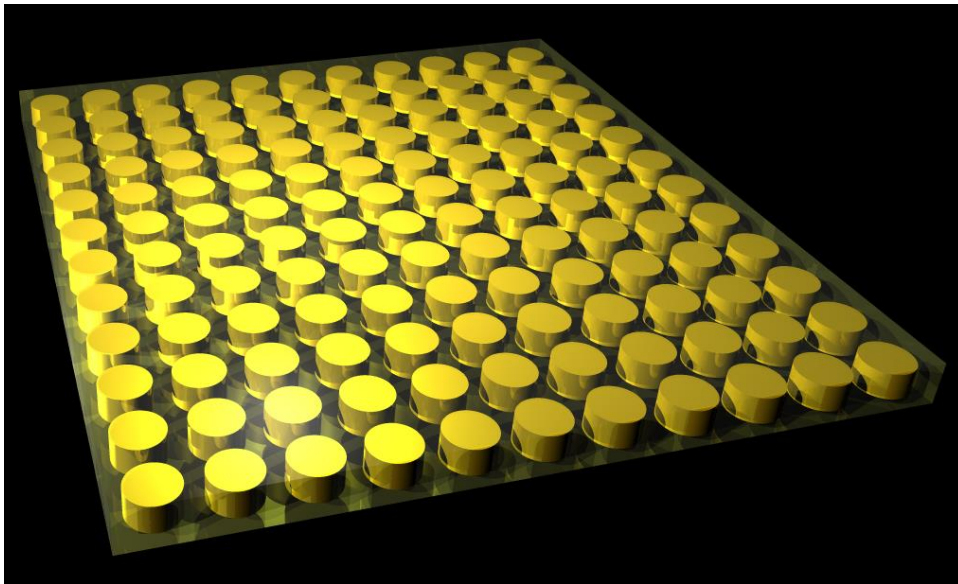


Fig. 14 Square array of subwavelength high refractive index cylinders embedded in a low-index host.

5. OPTIMIZING FREQUENCY DISPERSION

Metal-dielectric nanocomposites exhibit very complex photonic behavior even in the case of the simplest structures. An interplay between Bragg and plasmon-polariton interface phenomena generates a plethora of various electromagnetic modes. As an illustration, Fig. 15 shows a frequency dispersion of a simple one-dimensional metal-dielectric multilayer with only 3 metal-dielectric pairs. The structure is deposited on dielectric and surrounded by air or vacuum. Even such a basic plasmonic structure shows a surprising wealth of modes. Besides a bandgap one can observe different plasmonic modes (to the right of the light line), including those modes that exist within the bandgap and cross into the bands, as well as the negative group velocity modes.

Obviously, if we meet such a complex situation for a simple 1D plasmonic crystal, with increasing structural complexity (making nanoplasmonic structures in 2D and 3D), it should be possible to customize frequency dispersion of the obtained artificial materials to arrive at almost any desired group velocity in a given frequency/wave vector range. The idea is to adjust the parameters to minimize losses and maximize FOM for a given frequency range.

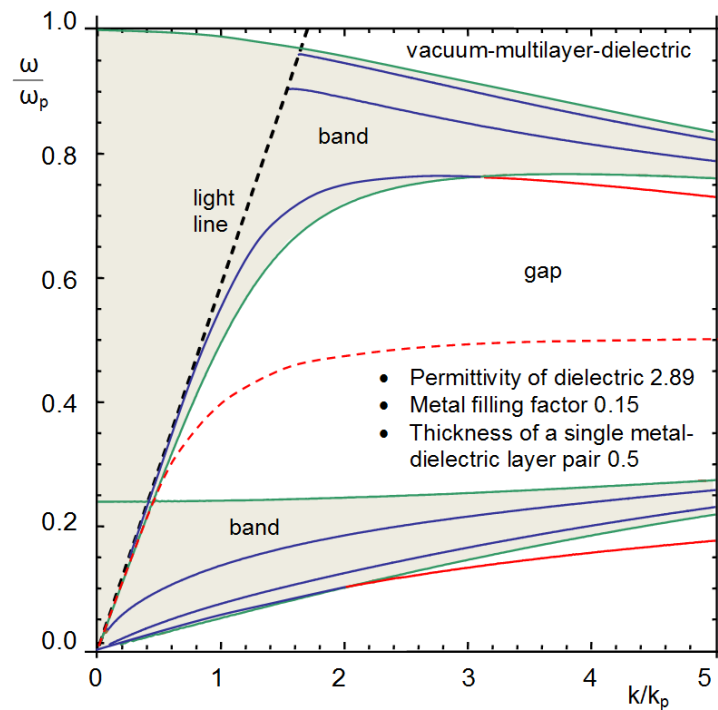


Fig. 15 Frequency dispersion of a simple three-layer pair metal-dielectric with vacuum ($n=1$) on top side and dielectric substrate $n=2.89$.

Now we give here an example of plasmonic metamaterials that can have strongly decreased losses. It is an old/new paradigm –materials with hyperbolic dispersion [44] (HM, hyperbolic metamaterials). The effect was first demonstrated in 1969, but only relatively recently attracted attention within the field of metamaterials. HM metallodielectric structures became a target of intensive research, among other reasons, because their absorption losses can be strongly reduced.

HM is a metamaterial designed to exhibit extreme optical anisotropy, with opposite signs of dielectric permittivity in two orthogonal directions

$$\varepsilon_n \cdot \varepsilon_t < 0 \quad (1)$$

$$\varepsilon_t = \varepsilon_x = \varepsilon_y, \varepsilon_n = \varepsilon_z \quad (2)$$

Hyperbolic dispersion for extraordinary waves:

$$k_t^2/\varepsilon_n + k_n^2/\varepsilon_t = k_0^2 \quad (3)$$

$$k_0^2 = \omega^2/c^2, k_t^2 = k_x^2 + k_y^2, k_n = k_z. \quad (4)$$

HM are much easier to fabricate than the well-known double-negative media (artificial composites that simultaneously have their effective permeability and permittivity below zero, i.e. negative refractive index metamaterials). A visual presentation of topological transformations in k -space which bring to hyperbolic dispersion is shown in Fig. 16.

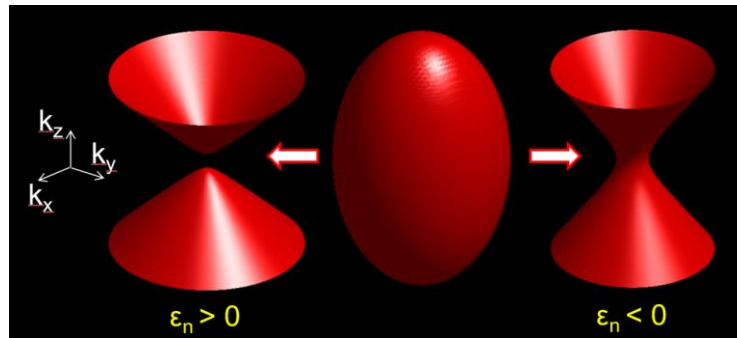


Fig. 16 Topological transitions in k -space: isofrequency surfaces for extraordinary waves in hyperbolic metamaterials.

Various implementations of hyperbolic metamaterials are illustrated in Fig.17. The simplest one is obviously a metal-dielectric multilayer whose isofrequency surfaces are hyperbolic. Other examples include multilayer fishnet metamaterials and their complementary structures, pillars made from alternating metal and dielectric layers. Finally, the most complex design presented in Fig. 17 is a sculpted metal-dielectric film – the superlens design.

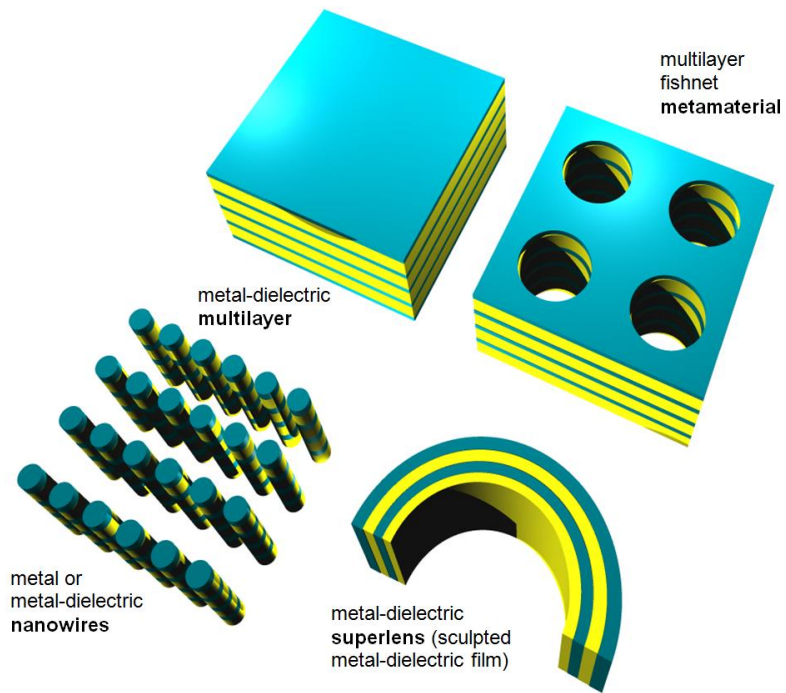


Fig. 17 Examples of hyperbolic metamaterials

Another type of structures that can be used to tailor optical absorption losses are the plasmonic hypercrystals. They can be defined as a periodic combination of hyperbolic medium with another medium (metal, dielectric, metamaterial...) [45]. A general design of a hypercrystal is shown in Fig. 18.

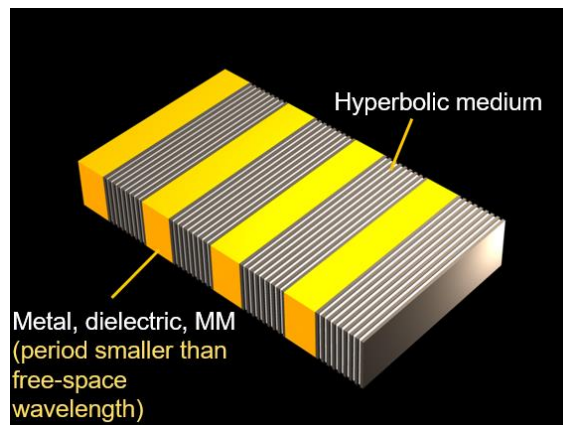


Fig. 18 General design of a hypercrystal

Dispersion of hyperbolic materials does not impose diffraction limit for TM waves (system unlimited by frequency!)

Bragg reflection in a hyperbolic photonic crystal ($d \sim \lambda_0$) leads to the appearance of optical Tamm surface states [7]. In hypercrystals the formation of PBGs (photonic bandgaps) persists in the subwavelength mode (metamaterial regime, $d \ll \lambda_0$)

Optical Tamm states in hypercrystals lead to high EM confinement (larger wave numbers) and simultaneously to lower absorption losses compared to surface plasmons polaritons.

Such behavior does not occur either in conventional PBG or in metamaterials.

Figures 19 and 20 show the frequency dispersion of the extinction coefficient $\text{Im}(k_n)d$ (absorption) in a hypercrystal in dependence on the normalized in-plane momentum ($k_{\parallel} = k_0$) for varying $\tau = 1/\gamma$ in lossy Drude model (Fig. 19).

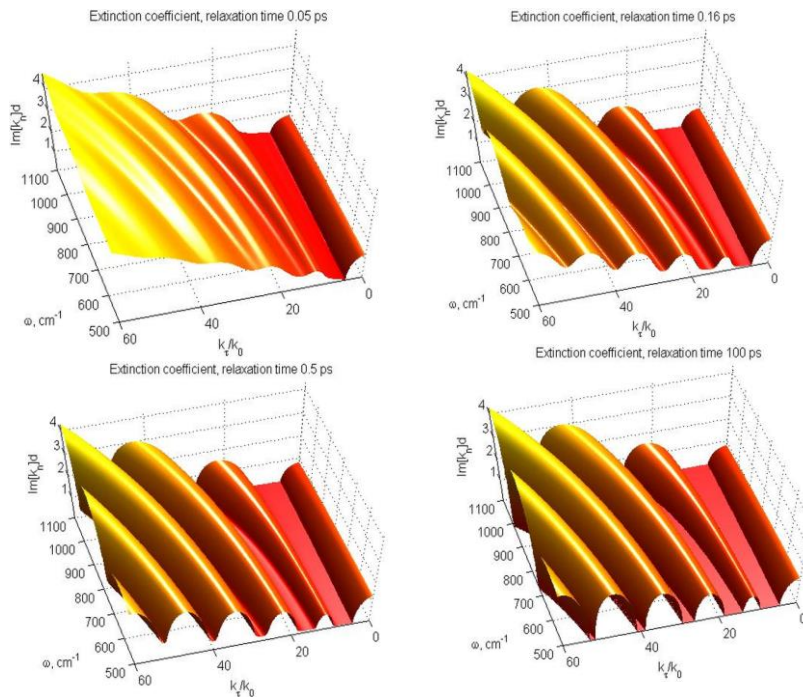


Fig. 19 Absorption in a hypercrystal for varying $\tau = 1/\gamma$ in lossy Drude model.

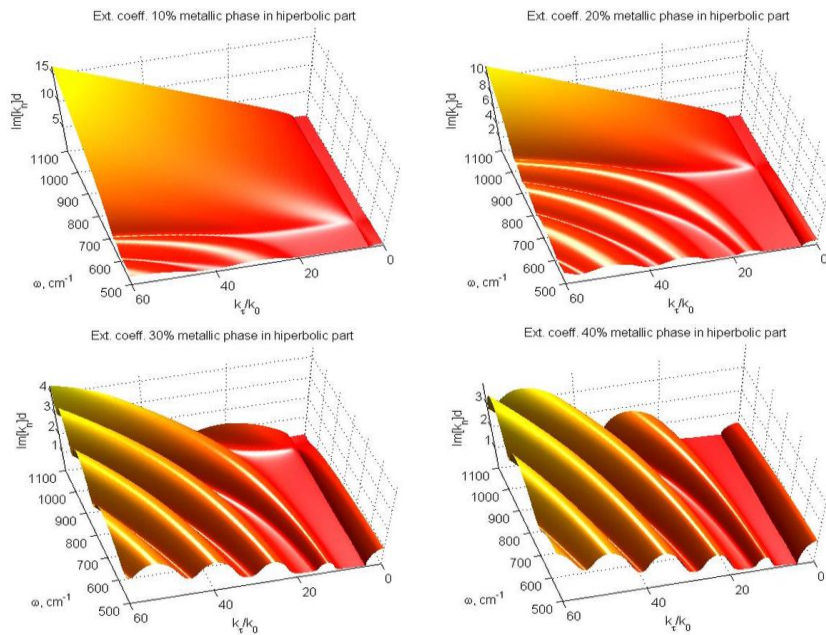


Fig. 20 Absorption in a hypercrystal for varying metal fraction in hyperbolic part.

6. CONCLUSION

Reaching low-loss or lossless nanophotonics & plasmonics is a holy grail of electromagnetics, photonics and transformation optics. Strategies include the use of alternative plasmonic materials, all-dielectric nanocomposites and optimization of dispersion and structure toward lower losses. Each of them holds its own promises and pitfalls. A winning combination is not (yet) known, but may include a combination of two or more of the above.

A host of practical applications would benefit: transformation optics (including superlenses and hyperlenses, cloaking devices, superconcentrators, superabsorbers...) Elimination of losses is a crucial step toward merging electronics and photonics into super-compact, super-fast new generation of integrated circuitry.

Acknowledgement: *The paper is a part of the research funded by the Serbian Ministry of Education and Science within the projects TR32008, III45016 and ON171005, as well as by the Qatar National Research Fund within the projects NPRP 8-028-1-001 and NPRP 7-665-1-125.*

REFERENCES

- [1] U. Leonhardt, "Optical Conformal Mapping," *Science*, vol. 312, no. 5781, pp. 1777-1780, 2006.
- [2] Y. Liu, T. Zentgraf, G. Bartal, and X. Zhang, "Transformational plasmon optics," *Nano Lett.*, vol. 10, no. 6, pp. 1991-1997, 2010.
- [3] J. B. Pendry, D. Schurig, and D. R. Smith, "Controlling Electromagnetic Fields," *Science*, vol. 312, no. 5781, pp. 1780-1782, 2006.
- [4] W. Cai, and V. Shalaev, *Optical Metamaterials: Fundamentals and Applications*, Springer, Dordrecht, Germany, 2009.
- [5] S. A. Ramakrishna, and T. M. Grzegorzczuk, *Physics and Applications of Negative Refractive Index Materials*, SPIE Press Bellingham, WA & CRC Press, Taylor & Francis Group, Boca Raton FL, 2009.
- [6] M. I. Dyakonov, "New type of electromagnetic wave propagating at an interface," *Sov. Phys. JETP*, vol. 67, pp. 714-716, 1988.
- [7] G. Isić, S. Vuković, Z. Jakšić, and M. Belić, "Tamm plasmon modes on semi-infinite metallodielectric superlattices," *Scientific Reports*, vol. 7, no. 1, pp. 3746, 2017.
- [8] J. A. Polo Jr, and A. Lakhtakia, "Surface electromagnetic waves: A review," *Laser and Photonics Reviews*, vol. 5, no. 2, pp. 234-246, 2011.
- [9] J. Yang, M. Huang, C. Yang, Z. Xiao, and J. Peng, "Metamaterial electromagnetic concentrators with arbitrary geometries," *Opt. Express*, vol. 17, no. 22, pp. 19656-19661, 2009.
- [10] D. S. Wiersma, P. Bartolini, A. Lagendijk, and R. Righini, "Localization of light in a disordered medium," *Nature*, vol. 390, no. 6661, pp. 671-673, 1997.
- [11] N. I. Landy, S. Sajuyigbe, J. J. Mock, D. R. Smith, and W. J. Padilla, "Perfect metamaterial absorber," *Phys. Rev. Lett.*, vol. 100, no. 20, 2008.
- [12] N. Liu, M. Mesch, T. Weiss, M. Hentschel, and H. Giessen, "Infrared perfect absorber and its application as plasmonic sensor," *Nano Lett.*, vol. 10, no. 7, pp. 2342-2348, 2010.
- [13] J. Ng, H. Chen, and C. T. Chan, "Metamaterial frequency-selective superabsorber," *Opt. Lett.*, vol. 34, no. 5, pp. 644-646, 2009.
- [14] N. Fang, H. Lee, C. Sun, and X. Zhang, "Sub-diffraction-limited optical imaging with a silver superlens," *Science*, vol. 308, no. 5721, pp. 534-537, 2005.
- [15] Z. Liu, S. Durant, H. Lee, Y. Pikus, N. Fang, Y. Xiong, C. Sun, and X. Zhang, "Far-field optical superlens," *Nano Lett.*, vol. 7, no. 2, pp. 403-408, 2007.
- [16] J. B. Pendry, and D. R. Smith, "The quest for the superlens," *Sci. Am.*, vol. 295, no. 1, pp. 60-67, 2006.
- [17] Z. Jacob, L. V. Alekseyev, and E. Narimanov, "Optical hyperlens: Far-field imaging beyond the diffraction limit," *Opt. Express*, vol. 14, no. 18, pp. 8247-8256, 2006.
- [18] Z. Liu, H. Lee, Y. Xiong, C. Sun, and X. Zhang, "Far-field optical hyperlens magnifying sub-diffraction-limited objects," *Science*, vol. 315, no. 5819, pp. 1686, 2007.
- [19] E. E. Narimanov, and V. M. Shalaev, "Optics: Beyond diffraction," *Nature*, vol. 447, no. 7142, pp. 266-267, 2007.
- [20] W. Cai, U. K. Chettiar, A. V. Kildishev, and V. M. Shalaev, "Optical cloaking with metamaterials," *Nature Photonics*, vol. 1, no. 4, pp. 224-227, 2007.
- [21] T. Ergin, N. Stenger, P. Brenner, J. B. Pendry, and M. Wegener, "Three-dimensional invisibility cloak at optical wavelengths," *Science*, vol. 328, no. 5976, pp. 337-339, 2010.
- [22] E. Ozbay, "Plasmonics: Merging Photonics and Electronics at Nanoscale Dimensions," *Science*, vol. 311, no. 5758, pp. 189-193, 2006.
- [23] S. A. Maier, *Plasmonics: Fundamentals and Applications*, Springer Science+Business Media, New York, NY, 2007.
- [24] J. Brown, "Artificial dielectrics having refractive indices less than unity," *Proc. IEEE*, vol. 100, no. 4, pp. 51-62, 1953.
- [25] J. Brown, "Artificial dielectrics," *Progress in Dielectrics*, J. B. Birks, ed., pp. 193-225, Hoboken, New Jersey: Wiley, 1960.
- [26] S. M. Vuković, Z. Jakšić, and J. Matovic, "Plasmon modes on laminated nanomembrane-based waveguides," *J. Nanophotonics*, vol. 4, pp. 041770, 2010.
- [27] Z. Jakšić, and J. Matovic, "Functionalization of Artificial Freestanding Composite Nanomembranes," *Materials*, vol. 3, no. 1, pp. 165-200, 2010.
- [28] C. Jiang, S. Markutsya, Y. Pikus, and V. V. Tsukruk, "Freely suspended nanocomposite membranes as highly sensitive sensors," *Nature Mater.*, vol. 3, no. 10, pp. 721-728, 2004.
- [29] P. Berini, "Long-range surface plasmon polaritons," *Adv. Opt. Photon.*, vol. 1, no. 3, pp. 484-588, 2009.

- [30] P. Berini, R. Charbonneau, and N. Lahoud, "Long-range surface plasmons along membrane-supported metal stripes," *IEEE J. Sel. Top. Quant. Electr.*, vol. 14, no. 6, pp. 1479-1495, 2008.
- [31] A. Boltasseva, and H. A. Atwater, "Low-Loss Plasmonic Metamaterials," *Science*, vol. 331, no. 6015, pp. 290-291, 2011.
- [32] P. R. West, S. Ishii, G. V. Naik, N. K. Emani, V. Shalaev, and A. Boltasseva, "Searching for better plasmonic materials," *Laser & Photon. Rev.*, pp. 1-13, 2010.
- [33] S. Franzen, C. Rhodes, M. Cerruti, R. W. Gerber, M. Losego, J. P. Maria, and D. E. Aspnes, "Plasmonic phenomena in indium tin oxide and ITO-Au hybrid films," *Opt. Lett.*, vol. 34, no. 18, pp. 2867-2869, 2009.
- [34] Z. Fei, A. Rodin, G. Andreev, W. Bao, A. McLeod, M. Wagner, L. Zhang, Z. Zhao, M. Thiemens, and G. Dominguez, "Gate-tuning of graphene plasmons revealed by infrared nano-imaging," *Nature*, vol. 487, no. 7405, pp. 82, 2012.
- [35] A. Grigorenko, M. Polini, and K. Novoselov, "Graphene plasmonics," *Nature Photonics*, vol. 6, no. 11, pp. 749, 2012.
- [36] J. M. Luther, P. K. Jain, T. Ewers, and A. P. Alivisatos, "Localized surface plasmon resonances arising from free carriers in doped quantum dots," *Nature Mater.*, vol. 10, no. 5, pp. 361, 2011.
- [37] S. Jahani, and Z. Jacob, "All-dielectric metamaterials," *Nature Nanotech.*, vol. 11, no. 1, pp. 23-36, 2016.
- [38] A. I. Kuznetsov, A. E. Miroshnichenko, M. L. Brongersma, Y. S. Kivshar, and B. Luk'yanchuk, "Optically resonant dielectric nanostructures," *Science*, vol. 354, no. 6314, 2016.
- [39] P. Spinelli, M. A. Verschuuren, and A. Polman, "Broadband omnidirectional antireflection coating based on subwavelength surface Mie resonators," *Nature Comm.*, vol. 3, 2012.
- [40] M. Quinten, *Optical Properties of Nanoparticle Systems: Mie and Beyond*, Wiley-VCH, Weinheim, Germany, 2011.
- [41] M. Schmid, R. Klenk, M. C. Lux-Steiner, M. Topič, and J. Krč, "Modeling plasmonic scattering combined with thin-film optics," *Nanotechnology*, vol. 22, no. 2, pp. 025204.1-10, 2010.
- [42] Z. Jakšić, M. Obradov, S. Vuković, and M. Belić, "Plasmonic enhancement of light trapping in photodetectors," *Facta Universitatis, Series: Electronics and Energetics*, vol. 27, no. 2, pp. 183-203, 2014.
- [43] A. Epstein, and G. V. Eleftheriades, "Huygens' metasurfaces via the equivalence principle: design and applications," *JOSA B*, vol. 33, no. 2, pp. A31-A50, 2016.
- [44] A. Poddubny, I. Iorsh, P. Belov, and Y. Kivshar, "Hyperbolic metamaterials," *Nature Photonics*, vol. 7, no. 12, pp. 948-957, 2013.
- [45] E. E. Narimanov, "Photonic hypercrystals," *Physical Review X*, vol. 4, no. 4, 2014.